Stable Polymorphs Crystallized Directly under Thermodynamic Control in Three-Dimensional Nanoconfinement: A Generic Methodology

ARTICLE *in* CRYSTAL GROWTH & DESIGN · JANUARY 2011

Impact Factor: 4.89 · DOI: 10.1021/cg101200f

4 AUTHORS, INCLUDING:

Catherine E Nicholson
Durham University
10 PUBLICATIONS **110** CITATIONS
SEE PROFILE

Cen Chen
Durham University
3 PUBLICATIONS **26** CITATIONS
SEE PROFILE

Sharon J Cooper
Durham University
36 PUBLICATIONS **861** CITATIONS
SEE PROFILE

DOI: 10.1021/cg101200f

CRYSTAL GROWTH & DESIGN
Communication
2011, Vol. 11
363–366

Stable Polymorphs Crystallized Directly under Thermodynamic Control in Three-Dimensional Nanoconfinement: A Generic Methodology

Catherine E. Nicholson,[†] Cen Chen,[†] Budhika Mendis,[‡] and Sharon J. Cooper*[,†]

[†]*Department of Chemistry, University Science Laboratories, South Road, Durham, DH1 3LE, U.K., and* [‡]*Department of Physics, Durham University, South Road, Durham DH1 3LE, U.K.*

Received September 9, 2010; Revised Manuscript Received December 18, 2010

ABSTRACT: Thermodynamic control of crystallization has been achieved to produce stable polymorphs directly by using three-dimensional (3D) nanoconfinement in microemulsions. The theoretical basis for thermodynamic control of crystallization using 3D nanoconfinement is outlined. Our approach leap-frogs the usual metastable polymorph pathway because crystallization becomes governed by the ability to form stable nuclei, rather than critical nuclei. The generality of this approach is demonstrated by crystallizing the stable polymorph of three "problem" compounds from microemulsions under conditions yielding metastable forms in bulk solution. The polymorphic compounds are mefenamic acid (2-[(2,3-(dimethylphenyl)amino] benzoic acid), glycine (aminoethanoic acid), and the highly polymorphic 5-methyl-2-[(2-nitrophenyl) amino]-3-thiophenecarbonitrile, commonly known as ROY because of its red, orange, and yellow polymorphs. Application of this methodology should prevent another Ritonavir-type disaster, whereby a marketed drug transforms into a more stable form, reducing its bioavailability and effectiveness. The lowest energy nuclei selectively grow in our approach. Consequently, this also provides a generic method for producing higher crystallinity materials, which may prove beneficial for crystallizing proteins and inorganic nanocrystals.

In 1897 Ostwald coined his now famous rule of stages[1] stating that metastable polymorphs crystallize initially. The metastable polymorphs may then transform into more stable forms, but the time-scale involved is highly variable. Ostwald's rule of stages is often obeyed because crystallization is typically under kinetic, rather than thermodynamic, control. Consequently, and despite extensive screening tests, pharmaceutical companies cannot guarantee their marketed drug will not transform into a more stable polymorph with a lower bioavailability, making the drug less effective. This happened to the infamous anti-AIDS drug Ritonavir in 1998, forcing the removal of the drug from the market and its reformulation,[2] to the cost of several hundred million dollars. In this paper, we show how to "leap-frog" Ostwald's rule of stages by using the three-dimensional (3D) nanoconfinement of microemulsions to exert thermodynamic control over crystallization. Microemulsions[3] with 3D nanoconfinement comprise thermodynamically stable nanoscale droplets of a liquid/solution (the confined phase), dispersed in an immiscible liquid/solution (the continuous phase), with surfactant molecules residing at the droplet interface. The droplet size is typically 2−10 nm, with a relatively narrow polydispersity of $\sigma_R/R_{max} \approx 0.1-0.2$, where σ_R is the Gaussian distribution standard deviation and R_{max} is the modal droplet radius.[4] Here we use the term "microemulsion" to also encompass swollen micelles. Crystallization in microemulsions has been studied previously to produce inorganic nanoparticles[5,6] and particular polymorphs through specific surfactant−polymorph interactions.[7−9] This study, however, reveals how generic thermodynamic control is achievable, to enable direct crystallization of stable polymorphs.

Crystallization occurs from solutions that are supersaturated, that is, that have solute concentrations above their saturation values, c_{sat}, where c_{sat} is the solute concentration in equilibrium with macroscopic crystals (Supporting Information, section 2.1). For an ideal solution, the supersaturation is $\Delta\mu = kT \ln(c/c_{sat})$, where k is the Boltzmann constant, T is temperature, and c/c_{sat}, the ratio of the solute concentration compared to its saturation value, is known as the supersaturation ratio. Crystallization involves two stages: nucleation and crystal growth. Nucleation consists of overcoming the crystallization energy barrier, ΔF^*, arising from creating an interface between the nucleus and solution. Crystal nuclei corresponding to this energy maximum are termed critical nuclei. These critical nuclei grow until the supersaturation is relieved. The nucleation barrier, ΔF^*, for the stable polymorph is higher than for a metastable polymorph if Ostwald's rule of stages is obeyed. An example is shown schematically in Figure 1a for a polymorphic compound with stable polymorph A and metastable polymorph B. In such a system, B will tend to crystallize first and the existence of stable polymorph A may never be known. However, we can "leap-frog" Ostwald's rule of stages and crystallize the stable polymorph directly by using a 3D nanoconfined solution. The scientific rationale is as follows.

For crystallization from 3D nanoconfined solutions, a minimum in the free energy arises due to the decrease in solute concentration, and hence supersaturation, as the new crystal phase grows.[10,11] In particular, adopting a classical homogeneous nucleation approach for crystallization from an ideal solution in a spherical confining volume, V, the Helmholtz free energy change, ΔF, to produce a nuclei containing n molecules would be given by[12]

$$\Delta F = -n\Delta\mu + \gamma A + NkT\left\{\ln\left(1-\frac{v}{Vv_c c_0}\right) - \frac{1}{v_c c_0}\ln\left(1-\frac{v}{V}\right)\right\}$$

where $\Delta\mu = kT \ln(c/c_{sat})$ is the supersaturation at that nucleus size with $c = (N-n)/(V-v) = c_0(1-(v/(Vv_c c_0)))(1/(1-v/V))$, γ and A are the interfacial tension[13] and surface area, respectively, at the nucleus−solution interface, N is the initial number of solute molecules when $n = 0$, v is the nucleus volume, v_c is the molecular volume of the crystalline species, and c_0 is the initial solute concentration when $n = 0$. The first two terms comprise those expected from classical nucleation theory for crystallization from unconfined volumes, while the third term provides the correction due to the supersaturation depletion as the nucleus grows.

The free energy change at the minimum is denoted ΔF^*_{min}, and the corresponding nucleus size is Δr^*_{min} (Figure 1b). The stable polymorph is the least soluble, so polymorph A can grow to larger sizes than metastable B before its supersaturation is depleted, thus $r^*_{min,A} > r^*_{min,B}$. This larger size and the polymorph's greater stability mean we would typically expect $\Delta F^*_{min,A} < F^*_{min,B}$.

*Department of Chemistry, University Science Laboratories, South Road, Durham, DH1 3LE, UK. Tel: +44 (0)191 334 2098. Fax: +44 (0)191 334 2051. E-mail: sharon.cooper@durham.ac.uk.

Published on Web 01/05/2011

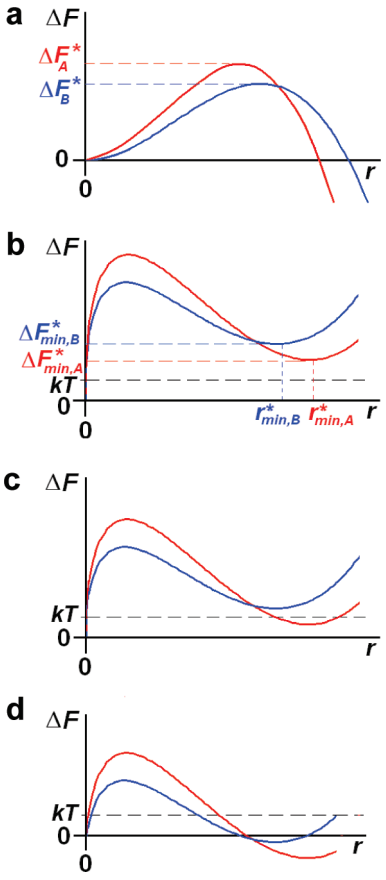

Figure 1. Example graphs of free energy change, ΔF vs nucleus size, r for systems crystallizing from (a) bulk solution and (b), (c), (d), a 3D nanoconfined solution. Polymorph A (red) is stable while polymorph B (blue) is metastable. In (a) the bulk solution case, Ostwald's rule of stages is obeyed with polymorph B tending to crystallize first. In (b) crystallization is disfavored and the system is stabilized due to 3D nanoconfinement. In (c) thermodynamic control over crystallization is achieved as only polymorph A will tend to crystallize, but thermodynamic control will typically be lost for system (d), with both polymorphs tending to crystallize.

The population of r^*_{min} nuclei at equilibrium depends upon the Boltzmann factor, $\exp(-\Delta F^*_{min}/kT)$, and so will be sizable for $\Delta F^*_{min} \leq kT$, with (near) stable nuclei produced. Consequently, thermodynamic control is obtained for 3D nanoconfinements when only the stable polymorph A has $\Delta F^*_{min} \leq kT$ (Figure 1c), as then only this form will have a sizable population of (near) stable nuclei, provided its nucleation energy barrier is surmountable. The latter can be ensured by crystallizing from sufficiently small droplets, since these require such high initial supersaturations to enable (near) stable nuclei to form.

For microemulsions, there will be a range of droplet sizes and concentrations of solute molecules within the droplets. Consequently, thermodynamic control is attainable when droplets with the largest supersaturations and sizes contain (near) stable nuclei of the stable polymorph, but negligible quantities of the other forms. The key to finding this specific condition is to initially obtain a supersaturated system that is stabilized solely due to 3D nanoconfinement. Such a system has sufficient supersaturation within the 3D nanoconfinement to form critical nuclei, but the population of any larger (near) stable nuclei is negligible, that is, $\Delta F^*_{min} \gg kT$ even for droplets with the largest supersaturations and sizes (Figure 1b). This system is characterized by crystallization being severely hindered/prevented compared to the analogous unconfined system. Crystallization under thermodynamic control is then induced by increasing the supersaturation until (near) stable nuclei of only the stable polymorph form (Figure 1c). With further supersaturation increases, thermodynamic control can be retained provided the reverse process of r^*_{min} nuclei dissolution is sufficiently rapid that the equilibrium concentration of r^*_{min} nuclei can be established. This depends upon the magnitude of $\Delta F^* - \Delta F^*_{min}$. If the nucleation barrier ΔF^* is surmountable but $\Delta F^* - \Delta F^*_{min} \gg kT$, that is, $\Delta F^*_{min} < 0$ as in Figure 1d, then the dissolution rate of the r^*_{min} nuclei will be slow. The relative proportion of the $r^*_{min,A}$ and $r^*_{min,B}$ will then depend principally upon their rates of formation; the system will come under kinetic control and thermodynamic control will be lost (Figure 1d).

The (near) stable nuclei within the microemulsion droplets grow to larger dimensions by the following process. Collisions occur between the droplets and the most energetic of these cause transient droplet dimers to form, with accompanying exchange of interior content.[5] This enables the (near) stable nuclei to gain access to more molecules and grow until they become larger than the droplets and so are no longer confined. Further growth can then occur to produce ~μm or millimeter-sized crystals either from the typically miniscule concentration of their molecules in the continuous phase, or via contact with the interior of the microemulsion droplets arising from energetic collisions. Although not observed here, a metastable polymorph could potentially have the lowest ΔF^*_{min} if, for example, it was sufficiently stabilized by the surrounding solvent. This possibility can be readily checked by using a different solvent, or by gradually increasing the supersaturation until crystals/nanocrystals of more than one polymorph crystallize, so that all low energy polymorphs can be identified. We demonstrate the generality of our thermodynamic control for three "problem" polymorphic compounds, mefenamic acid, glycine, and ROY, which have well-known difficulty in crystallizing their stable polymorphs.

Mefenamic acid has two polymorphs, Form I, which is stable at ambient temperatures, and metastable Form II. Crystallization of mefenamic acid from bulk DMF produces only Form II, irrespective of the crystallization rate or temperature.[14−16] In contrast, Form I nanocrystals were evident from transmission electron microscopy (TEM) analysis on DMF microemulsions cooled from 50 to 8 °C over 12 h and then left at 8 °C for 12 h (Figure 2a,b). These microemulsions had mean hydrophilic core radii of 1.6 nm and mean initial supersaturation ratios, $(\overline{c/c_{sat}})_{initial}$ with respect to Form I of 4.1−7.0. Crystallization was only just possible for $(\overline{c/c_{sat}})_{initial} = 4.1$. The nanocrystals were predominantly of Form I for $(\overline{c/c_{sat}})_{initial} = 4.1-5.3$, but thereafter Form II nanocrystals become increasingly evident, with $(\overline{c/c_{sat}})_{initial} \geq 6.1$ resulting in predominantly Form II. This finding was confirmed by in situ Raman spectroscopy on ~mm-sized crystals, with Form I and Form II crystals obtainable from DMF microemulsions and bulk DMF solution, respectively (Figure 2c). Form I has characteristic peaks at 623, 702, and 1581 cm^{-1}, while Form II has characteristic peaks at 631, 694, and 1573 cm^{-1}. The AOT (sodium dioctyl sulfosuccinate) surfactant used in the microemulsions does not induce Form I crystallization (Supporting Information, section 2.2), so its occurrence is not attributable to the surfactant.

Glycine has three polymorphs, α, β, and γ, which are obtainable under ambient conditions. The γ-form is the stable form, but was only discovered in 1954, over 40 years after the α-polymorph.[17] It is extremely difficult to obtain the γ-form from neutral aqueous solution unless, for example, specific additives[7,8,18−20] or very low supersaturations[21] are employed. This difficulty arises from the small stability difference of ≈0.2 kJ mol^{-1} between the bulk γ- and α-forms at ambient temperatures[22,23] and because the γ-form grows 500 times more slowly than the α-form in aqueous solution.[23] The microemulsions from which glycine was crystallized used the surfactants Span 80 (sorbitan monooleate) and Brij 30 (polyethylene glycol dodecyl

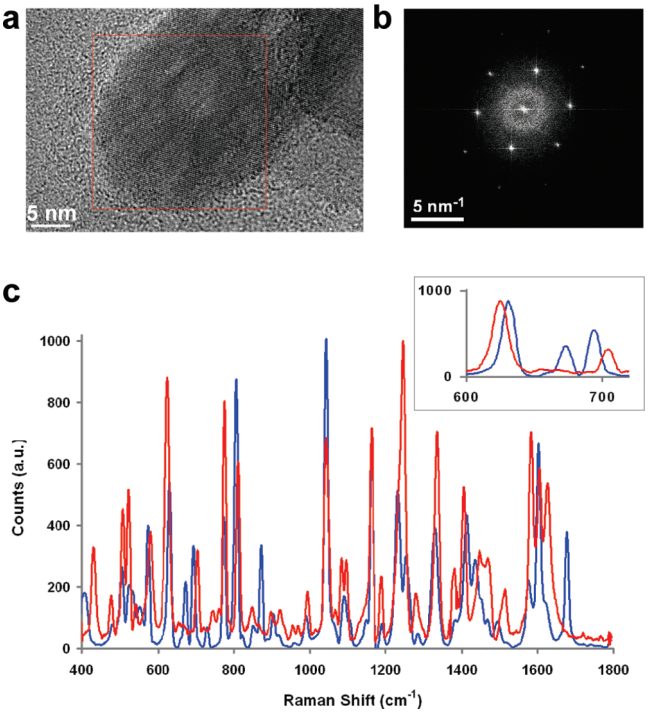

Figure 2. (a) High-resolution TEM image from an 8 °C mefenamic acid-in-DMF microemulsion of droplet size 1.6 nm with $(\overline{c/c_{sat}})_{initial}$ = 4.7, 1 day after cooling to 8 °C showing a ~20 nm nanocrystal within a mefenamic acid nanocrystal cluster. (b) Fourier transform of the red boxed region in (A) showing a "diffraction pattern" consistent with the Form I [$\bar{1}$11] zone axis. (c) In situ Raman spectra from 400 to 1800 cm^{-1} showing Form I in red crystallized from a DMF microemulsion with $(\overline{c/c_{sat}})_{initial}$ = 5.3 compared to Form II in blue crystallized from bulk DMF. The inset shows the 600−720 cm^{-1} region.

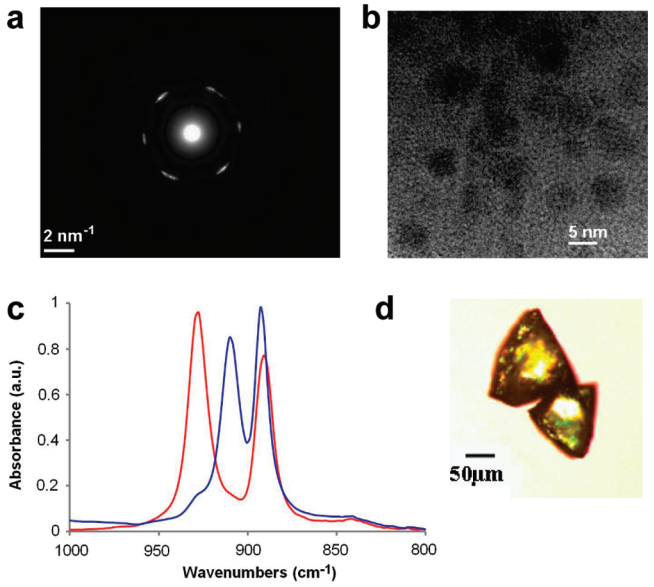

Figure 3. (a) A selected area electron diffraction pattern from a cluster of glycine γ-nanocrystals grown in 2 days from the mixed microemulsion with $(\overline{c/c_{sat}})_{initial}$ = 2.3; the hexagonal symmetry from the [001] zone axis of the γ-polymorph is readily seen. The Bragg peaks appear as arcs due to slight in-plane misorientation of the γ-nanocrystals. (b) A high resolution image of part of the cluster showing small ≈5 nm nanocrystals. (c) ATR-FTIR spectra from 1000 to 800 cm^{-1} showing γ-crystals (red) from the same microemulsion system aged 3 weeks compared to the α-crystals (blue) obtained from the mixed microemulsion when $(\overline{c/c_{sat}})_{initial}$ is higher at 2.9. (d) Optical micrograph of γ-crystals grown from a mixed microemulsion with $(\overline{c/c_{sat}})_{initial}$ = 2.3.

ether), which are known to induce crystallization of metastable forms at planar interfaces or in aqueous emulsions.[7,24,25] Hence, obtaining the stable γ-form from these microemulsions was a stringent test of our hypothesis. Nevertheless, we obtained the γ-form as the sole/majority product by adding aqueous methanol microemulsions to aqueous glycine microemulsions in quantities just sufficient to cause crystallization. Methanol is a poorer solvent for glycine than water, and so on mixing the microemulsions, a relatively rapid (i.e., ~ms to s)[5] equilibration of the water and methanol between droplets occurred to give droplets with a mean hydrophilic core radius of 3.6 nm and $(\overline{c/c_{sat}})_{initial}$ = 2.0−2.3 with respect to γ-glycine. TEM analysis showed that predominantly γ-nanocrystals of size ≈ 5 nm had grown 48 h after mixing the microemulsions (Figure 3a,b). After 3 weeks, the ~mm-sized γ-crystals were analyzed by attenuated total reflectance-Fourier transform infrared (ATR-FTIR) spectroscopy (Figure 3c). Characteristic peaks for γ- and α-crystals occur at 929 and 910 cm^{-1}, respectively. Figure 3d provides an optical micrograph showing two γ-crystals grown from the $(\overline{c/c_{sat}})_{initial}$ = 2.3 system. Increasing the glycine concentration above the minimum required for crystallization led to increasing proportions of α-glycine, with little/no γ-form observable for $(\overline{c/c_{sat}})_{initial}$ > 2.5.

ROY has 10 known polymorphs. The large number of polymorphs and their relatively small energy differences means that polymorphic control for ROY can be difficult[26] without specific additives.[27,28] Nevertheless, the stable yellow prism (Y) form was obtained selectively from microemulsions containing ROY mass fractions up to 0.15 in toluene on adding the poorer solvent heptane to give heptane/toluene volume ratios of 2:1. This corresponded to $(\overline{c/c_{sat}})_{initial}$ up to 24 with respect to the Y form, much greater than the $(\overline{c/c_{sat}})_{initial}$ ~ 10 value at which crystallization is first observable, and resulted in Y crystals being visible within a few hours of preparing the microemulsions. The microemulsions were stabilized with the surfactant Igepal CA720 (polyoxyethylene (12) isooctylphenyl ether), which does not aid Y crystallization (Supporting Information, section 2.2), and had a mean hydrophobic core radius of 2.8 nm. In contrast, the corresponding 0.15 mass fraction bulk experiments (Supporting Information, section 2.2) produce any combination of yellow needles (YN), red prisms (R), orange needles (ON), or Y crystals (Figure 4a). Figure 4b compares the ATR-FTIR spectra of the Y polymorph that crystallizes in the microemulsions to the metastable forms obtained predominantly in the bulk. Characteristic peaks occur at 2232, 2221, and 2210 cm^{-1} for the Y, YN, and R forms, respectively. ROY differs from mefenamic acid and glycine in that crystallization of the stable polymorph involves neither a large nucleation barrier nor a slow growth rate. Consequently, the stable form is obtained from microemulsions even when supersaturations much larger than the minimum required for crystallization are employed.

For the mefenamic acid, glycine, and ROY microemulsions that produced stable polymorphs, the mean number of solute molecules within each droplet was only ≈2, 5, and 2−5, respectively. However, because the (near) stable nuclei only arise in the largest droplets with the largest supersaturations, these nuclei will contain many more molecules than these mean values. An estimate for the glycine system, given the 0.2 kJ mol^{-1} free energy difference between the γ- and α-polymorphs, suggests thermodynamic preference will arise for (near) stable nuclei containing ~20−30 molecules. Each (near) stable nuclei will be surrounded by a slightly supersaturated solution containing ~3 glycine molecules, given the lower stability of the nuclei compared to its bulk crystal. Consequently, (near) stable nuclei are only likely to arise in droplets containing ~23−33 glycine molecules.

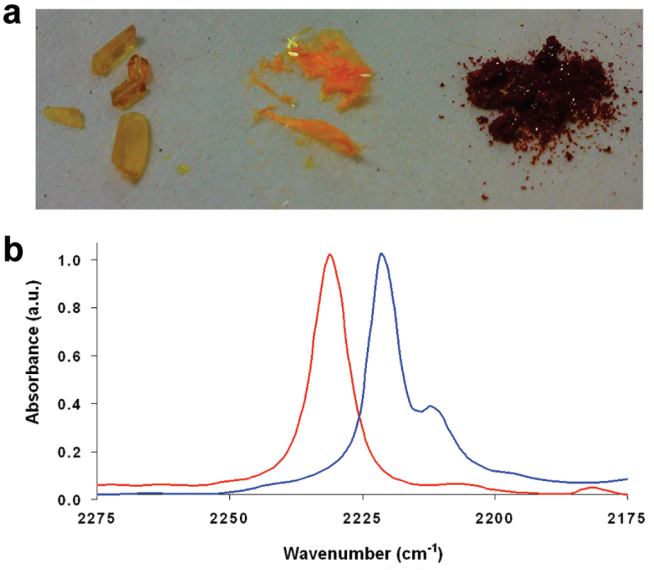

Figure 4. (a) ROY Y, ON, and R crystals grown from bulk experiments. (b) ATR-FTIR spectrum from 2275 to 2175 cm^{-1} of the stable ROY Y form obtained from 2:1 heptane/toluene microemulsions with 0.15 mass fraction ROY in toluene (red) compared to the spectrum obtained from a corresponding 2:1 heptane/toluene bulk crystallization (blue) showing YN with a minority of R crystals. Note that repeats of the bulk experiment could also produce Y and ON crystals.

If a Poisson distribution of glycine molecules among the droplets is assumed, then the proportion of droplets comprising such (near) stable nuclei is $< 10^{-8}$.

The ability of the (near) stable nuclei to determine the polymorphic outcome shows they contain sufficient crystal structure to ensure that outcome. This does not mean "amorphous" or less-structured nuclei do not form, just that their stability, and hence population, is lower. We would maintain that several nucleation pathways are possible, with the dominant pathway(s) determined by the crystallization conditions. In particular, the schematic Figure 1 implies a "classical" nucleation route encompassing a single energy barrier, but thermodynamic control via 3D nanoconfinement is also applicable to nonclassical crystallization comprising two-step nucleation[29] and precritical clusters residing in local energy minima,[30] since it is the ability to obtain (near) stable nuclei of only the stable polymorph, rather than the nucleation pathway, which ensures the thermodynamic control.

Thermodynamic control is achieved through 3D nanoconfinement by using the lowest supersaturations necessary to induce crystallization. The mefenamic acid and glycine cases show that the stable polymorph is produced when it is not achievable from bulk solution whether due to a high nucleation barrier and/or slow growth rate. The ability to crystallize stable polymorphs that have high nucleation barriers, in particular, is an important advance, since methods such as those using membrane crystallization[21] and polymeric heteronuclei[28] can only crystallize the stable polymorph if its nucleation barrier is low. Thus, our approach provides the generic capability of crystallizing stable polymorphs directly, necessary to prevent another Ritonavir-type crisis. Crystallization is ubiquitous. Hence, this generic ability to obtain stable polymorphs and higher crystallinity materials could potentially find uses in fields as diverse as proteinology, optoelectronics, and pharmaceuticals.

Acknowledgment. We thank C. Bain and M. Wilson for critical reading and discussions on the manuscript. The work is supported by the UK Engineering and Physical Sciences Research Council Grant No. EP/D070228/01.

Supporting Information Available: Experimental details and characterization techniques. Solubility of mefenamic acid, glycine, and ROY in the microemulsions. Control bulk crystallization experiments. SAXS results and analysis. This information is available free of charge via the Internet at http://pubs.acs.org.

References

(1) Ostwald, W. *Z. Phys. Chem.* **1897**, *22*, 289–330.
(2) Chemburkar, S. R.; Bauer, J.; Deming, K.; Spiwek, H.; Patel, K.; Morris, J.; Henry, R.; Spanton, S.; Dziki, W.; Porter, W.; Quick, J.; Bauer, P; Donaubauer, J.; B.; Narayanan, B. A.; Soldani, M.; Riley, D.; McFarland, K. *Org. Process Res. Dev.* **2000**, *4*, 413–417.
(3) The terminology "microemulsion" is confusing since the droplet sizes are ~nm, not μm, but the terminology was adopted well before the droplet sizes were known.
(4) Eriksson, J. C.; Ljunggren, S. *Langmuir* **1995**, *11*, 1145–1153.
(5) López-Quintela, M. A.; Tojo, C.; Blanco, M. C.; García Rio, L.; Leis, J. R. *Curr. Opin. Colloid Interface Sci.* **2004**, *9*, 264–278.
(6) Henle, J.; Simon, P.; Frenzel, A.; Scholz, S.; Kaskel, S. *Chem. Mater.* **2007**, *19*, 366–373.
(7) Allen, K.; Davey, R. J.; Ferrari, E.; Towler, C.; Tiddy, G. *Cryst. Growth Des.* **2002**, *2*, 523–527.
(8) Yano, J.; Füredi-Milhofer, H.; Wachtel, E.; Garti, N. *Langmuir* **2000**, *16*, 10005–10014.
(9) Füredi-Milhofer, H.; Garti, N.; Kamyshny, A. *J. Cryst. Growth* **1999**, *198/199*, 1365–1370.
(10) Reguera, D.; Bowles, R. K.; Djikaev, Y.; Reiss, H. *J. Chem. Phys.* **2003**, *118*, 340–353.
(11) Shirinyan, A. S.; Wautelet, M. *Mater. Sci. Eng., C* **2006**, *26*, 735–738.
(12) Cooper, S. J.; Nicholson, C. E.; Lui, J. *J. Chem. Phys.* **2008**, *129*, 124715.
(13) The interfacial tension for these ~nm nuclei should be treated as measuring the undersaturation of bonding across an interface, since this descriptor remains valid at the molecular level. Its value will vary with the nucleus size and is likely to differ significantly from the measurable macroscopic value.
(14) Alvarez, A. J.; Singh, A.; Myerson, A. S. *Cryst. Growth Des.* **2009**, *9*, 4181–4188.
(15) Aguiar, A. J.; Zelmer, J. E. *J. Pharm. Sci.* **1969**, *58*, 983–987.
(16) Cesur, S.; Gokbel, S. *Cryst. Res. Technol.* **2008**, *43*, 720–728.
(17) Towler, C. S.; Davey, R. J.; Lancaster, R. W.; Price, C. J. *J. Am. Chem. Soc.* **2004**, *126*, 13347–13353.
(18) Poornachary, S. K.; Chow, P. S.; Tan, R. B. H. *Cryst. Growth Des.* **2008**, *8*, 179–185.
(19) Weissbuch, I.; Leiseorowitz, L.; Lahav, M. *Adv. Mater.* **1994**, *6*, 952–956.
(20) Srinivasan, K. *J. Cryst. Growth* **2008**, *311*, 156–162.
(21) Di Profio, G.; Tucci, S.; Curcio, E.; Drioli, E. *Cryst. Growth Des.* **2007**, *7*, 526–530.
(22) Boldyreva, E. V.; Drebushchak, T. N.; Shakhtshneider, T. P.; Sowa, H.; Ahsbahs, H.; Goryainov, S. V.; Ivashevskaya, S. N.; Kolesnik, E. N.; Drebushchak, V. A.; Burgina, E. B. *ARKIVOC* **2004**, *xii*, 128–155.
(23) Chew, J. W.; Black, S. N.; Chow, P. S.; Tan, R. B. H.; Carpenter, K. J. *CrystEngComm* **2007**, *9*, 128–130.
(24) Nicholson, C. E.; Cooper, S. J.; Marcellin, C.; Jamieson, M. J. *J. Am. Chem. Soc.* **2005**, *127*, 11894–11895.
(25) Jamieson, M. J. Ph.D. Thesis, Durham University, 2004.
(26) Yu, L.; Stephenson, G. A.; Mitchell, C. A.; Bunnell, C. A.; Snorek, S. V.; Bowyer, J. J.; Borchardt, T. B.; Stowell, J. G.; Byrn, S. R. *J. Am. Chem. Soc.* **2000**, *122*, 585–591.
(27) Mitchell, C. A.; Yu, L.; Ward, M. D. *J. Am. Chem. Soc.* **2001**, *123*, 10830–10839.
(28) Price, C. P.; Grzesiak, A. L.; Matzger, A. J. *J. Am. Chem. Soc.* **2005**, *127*, 5512–5517.
(29) Kashchiev, D.; Vekilov, P. G.; Kolomeisky, A. B. *J. Chem. Phys.* **2005**, *122*, 244706.
(30) Gebauer, D.; Völkel, A.; Cölfen, H. *Science* **2008**, *322*, 1819–1822.